### Title

Kinetic Parameters of trans Scission by Extended HDV-like Ribozymes and the Prospect for the Discovery of Genomic trans-Cleaving RNAs




### Journal

Biochemistry, 57(9)

### ISSN

0006-2960



### Authors

Webb, Chiu-Ho T
Lupták, Andrej



### Publication Date

2018-03-06

### DOI

10.1021/acs.biochem.7b00789

Biochemistry

Article

Cite This: *Biochemistry* 2018, 57, 1440−1450

pubs.acs.org/biochemistry

# Kinetic Parameters of *trans* Scission by Extended HDV-like Ribozymes and the Prospect for the Discovery of Genomic *trans*-Cleaving RNAs

Chiu-Ho T. Webb[†,∥] and Andrej Lupták*[,†,‡,§]

[†]Department of Molecular Biology and Biochemistry, University of California—Irvine, Irvine, California 92697, United States

[‡]Department of Pharmaceutical Sciences, University of California—Irvine, Irvine, California 92697, United States

[§]Department of Chemistry, University of California—Irvine, Irvine, California 92697, United States

Supporting Information

**ABSTRACT:** Hepatitis delta virus (HDV)-like ribozymes are self-cleaving catalytic RNAs with a widespread distribution in nature and biological roles ranging from self-scission during rolling-circle replication in viroids to co-transcriptional processing of eukaryotic retrotransposons, among others. The ribozymes fold into a double pseudoknot with a common catalytic core motif and highly variable peripheral domains. Like other self-cleaving ribozymes, HDV-like ribozymes can be converted into *trans*-acting catalytic RNAs by bisecting the self-cleaving variants at non-essential loops. Here we explore the *trans*-cleaving activity of ribozymes derived from the largest examples of the ribozymes (drz-Agam-2 family), which contain an extended domain between the substrate strand and the rest of the RNA. When this peripheral domain is bisected at its distal end, the substrate strand is recognized through two helices, rather than just one 7 bp helix common among the HDV ribozymes, resulting in stronger binding and increased sequence specificity. Kinetic characterization of the extended *trans*-cleaving ribozyme revealed an efficient *trans*-cleaving system with a surprisingly high $K_M'$, supporting a model that includes a recently proposed activation barrier related to the assembly of the catalytically competent ribozyme. The ribozymes also exhibit a very long $k_{off}$ for the products (~2 weeks), resulting in a trade-off between sequence specificity and turnover. Finally, structure-based searches for the catalytic cores of these ribozymes in the genome of the mosquito *Anopheles gambiae*, combined with sequence searches for their putative substrates, revealed two potential ribozyme−substrate pairs that may represent examples of natural *trans*-cleaving ribozymes.

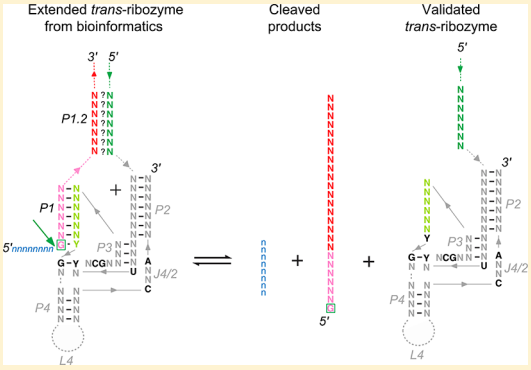


Self-cleaving ribozymes are small RNAs that fold into several distinct motifs and typically catalyze a single trans-esterification reaction, yielding a 2′−3′ cyclic phosphate and a 5′-hydroxyl at the scissile phosphodiester.[1,2] One of the most common self-cleaving motifs is the hepatitis delta virus (HDV) ribozyme, originating from a small single-stranded RNA helper virus of hepatitis B virus.[3] HDV harbors two structurally related self-cleaving ribozymes in its genome, one in the genomic and one in the complementary, antigenomic strand.[4−8] These ribozymes have been found in many other biological contexts, including in an intron of the mammalian *CPEB3* gene,[9] in a large number of eukaryotic retrotransposons,[10−13] in a noncoding RNA of a diplonemid,[14] and in untranslated mRNA regions of bacteria and an insect virus.[2,14] Their genomic distribution suggests diverse biological roles, although only a few have been elucidated to date.

HDV and HDV-like ribozymes consist of five paired regions that form two coaxial stacks (P1 stacks on P1.1 and P4, while P2 stacks on P3), which are linked by single-stranded joining (J) strands J1/2 and J4/2. Crystal structures of inhibited precursor and product states show that the genomic ribozyme folds into a nested double pseudoknot that constrains the overall structure and forms the active site of the ribozyme.[15−17] The ribozyme cleaves the RNA backbone at the base of the P1 helix, typically at a guanosine residue, and the active site is formed by the P3 helix, as well as the L3 and J4/2 strands.[15−17] A single nucleotide upstream and ~50 nucleotides (nts) downstream of the cleavage site are sufficient for self-scission.[7,18,19] HDV-like ribozymes have 6 or 7 bp in P1 and 3 bp in P3, while the P2 and P4 helices tend to show more length variation, mispairings, and insertions.[13,14,19,20] Moreover, the P4 helix is not absolutely required for activity, although it does seem to stabilize the active ribozyme.[19,21,22] Only a few positions in the sequence are invariant, including an active-site cytosine, a guanosine-pyrimidine base pair at the base of the P1 helix, an adenosine in J4/2 that forms an A-minor interaction with P3, and a G·U reverse wobble pair in L3 that forms the base of the P3 helix.[15−17,20]

**Received:** August 15, 2017
**Revised:** November 1, 2017
**Published:** February 1, 2018





DOI: 10.1021/acs.biochem.7b00789
*Biochemistry* 2018, 57, 1440−1450

A subgroup of HDV-like ribozymes, consisting of the largest examples of this family, includes a long and structured J1/2 insertion.[10,13,14] These peripheral domains were initially identified in drz-Agam-2-1, a fast-cleaving ribozyme from the African mosquito *Anopheles gambiae*, in which the stability of the peripheral domain correlated with the rate of self-scission.[23] The stability of the peripheral domain derives from the number of base pairs in the P1.2 helix and suggests that a precatalytic energy barrier is lowered when the P1.2 helix is longer, leading to highly active ribozymes with extended P1.2 domains. Motivated by this result and the possibility of creating a *trans*-cleaving complex that recognizes a long substrate strand, we sought to determine the activity of *trans*-cleaving ribozymes derived from the large *A. gambiae* self-cleaving RNAs.

Intermolecular scission can be derived from HDV-like self-cleaving ribozymes by bisecting the ribozymes between the P2 and P4 regions or J1/2 and P1 regions.[24,25] *trans*-cleaving HDV ribozymes were successfully used to cleave a target mRNA[26] and HCV RNA[27,28] *in vitro*. Similarly, influenza A,[29] telomerase,[30] HBV,[31] *pax-5B*,[32] and bacterial EF-Tu mRNA[33] have been targeted in cells, with the influenza A, *pax-5B*, and EF-Tu studies utilizing an extended ribozyme to recognize a longer target RNA. Because 15 or 16 bp is needed for specific substrate recognition in human cells,[34] *trans*-acting HDV ribozymes need to recognize the substrate RNA strand through interactions beyond the 7 bp P1 helix. The long J1/2 insertion region of drz-Agam-2-1 provides a good model for intermolecular scission, and the first part of this work presents the kinetic investigation of *trans*-acting drz-Agam-2-1.

While the *cis*-cleaving HDV-like ribozymes are widely distributed,[20] no genomic *trans*-acting ribozyme of this family has been identified. A *trans*-acting hammerhead ribozyme was proposed to exist in *Schistosoma mansoni*,[35] and a discontinuous hammerhead ribozyme was characterized in the *Clec2* gene in rodents,[36] indicating that *trans*-cleaving ribozymes may act in regulatory mechanisms. However, to the best of our knowledge, no systematic search for genomic *trans*-cleaving ribozymes has been presented. We therefore sought to develop a bioinformatic pipeline that identifies potential pairs of HDV-like *trans*-cleaving ribozymes and their substrates. Here we show that using drz-Agam-2-1 as a model and a systematic, structure-based search, *trans*-acting ribozymes and their potential substrates can be identified in *A. gambiae*.

## MATERIALS AND METHODS

**DNA Template Preparation.** Constructs were either amplified from the genome of *A. gambiae* or prepared by mutual priming of two synthetic, polyacrylamide gel electrophoresis (PAGE)-purified oligonucleotides. Primer extension was performed in a 100 $\mu$L reaction mixture containing the four dNTPs (0.2 mM each), 500 pmol of each primer, and 10 units of *Pfu* DNA polymerase (gift of G. Weiss, Department of Chemistry, University of California—Irvine). The primer-extension conditions were as follows: 94 °C for 1 min followed by two cycles of 50 °C for 30 s and 72 °C for 2 min. The polymerase chain reaction (PCR) conditions were as follows: 94 °C for 1 min, 50 °C for 30 s, and 72 °C for 2 min.

**Body-Labeled RNA Transcription.** RNA was transcribed at 37 °C for 1 h in a 5 $\mu$L volume containing 10 mM DTT, 2.5 mM GTP, 2.5 mM UTP, 2.5 mM CTP, 250 $\mu$M ATP, 1.25 $\mu$Ci of [$\alpha$-$^{32}$P]ATP (PerkinElmer), 7.75 mM $MgCl_2$, 1 unit of T7 RNA polymerase, and 0.5 pmol of DNA template.

**Nonlabeled RNA Transcription.** RNA was transcribed at 37 °C for 3 h in a 500 $\mu$L volume containing 10 mM DTT, 5 mM GTP, 5 mM UTP, 5 mM CTP, 5 mM ATP, 50 mM $MgCl_2$, 25 units of T7 RNA polymerase, and 25 pmol of DNA template. RNA was purified using denaturing (7 M urea) PAGE.

**$^{32}$P Labeling of RNA 3′-Termini.** RNA ligation was performed at 4 °C for 15 h in a volume of 20 $\mu$L, containing 20 pmol of RNA, RNA Ligase Buffer (NEB), an equal amount of [5′-$^{32}$P]cytidine 3′,5′-bisphosphate (PerkinElmer), and 1 unit of T4 RNA ligase (NEB). The 3′-labeled RNA was purified with a Sephadex G-25 spin column or PAGE.

**Cleaved 3′-Product Purification.** The substrate strand labeled with $^{32}$P at its 3′-terminus was incubated with an excess of ribozyme overnight, and the cleaved product was purified with PAGE.

**Cleavage Kinetics.** The ribozyme was preincubated with 1 mM $MgCl_2$ in a physiological-like buffer [140 mM KCl, 10 mM NaCl, and 50 mM Tris-HCl (pH 7.4)[9]] at 37 °C. Reactions were initiated by adding the 37 °C preincubated substrate to the ribozyme solution.[37] Aliquots (3 $\mu$L) taken at different time points were quenched with 6 $\mu$L of denaturing quench buffer [8 M urea, 20 mM EDTA, with 0.05% xylene cyanol, 0.1% bromophenol blue, and 1 mM Tris (pH 7.5)]. Denaturing PAGE of the products was exposed to phosphorimage screens (Molecular Dynamics) and analyzed by using a Typhoon phosphorimager and ImageQuant (GE Healthcare). The fraction intact was modeled using a biexponential decay and uncleaved residual function, with the faster of the two cleavage rates reported herein (eq 1).

$$k_{obs} = Ae^{-k_{fast}t} + Be^{-k_{slow}t} + C \quad (1)$$

where $k_{fast}$, $k_{slow}$, and $C$ correspond to the rate constant for the fastest-cleaving (and catalytically most competent) fraction ($A$) of the ribozyme population, the rate constant for a slow-cleaving fraction ($B$), and a fraction of the complexes that did not cleave ($C$), presumably due to misfolding, respectively.[38]

**Nondenaturing (native) PAGE.** Reaction kinetics were measured as in the experiments resolved on denaturing gels (described above), but the reaction buffer was supplemented with 10% glycerol, 0.05% xylene cyanol, and 0.1% bromophenol blue. At each time point, the aliquot was loaded directly onto a running 10% PAGE gel, containing TH buffer [33 mM Tris and 66 mM HEPES (pH 7.1)] and either 10 mM KCl or 1 mM $MgCl_2$.[39] Native PAGE was performed at a low power (5 W) to prevent gel heating and dissociation of complexes.

**Kinetic and Equilibrium Rate Constants of *trans*-Ribozymes.** The minimal kinetic mechanism for intermolecular drz-Agam-2-1 catalysis is outlined in Figure 1 and includes substrate association rate constant $k_1$ and dissociation rate constant $k_{-1}$, catalytic rate constant $k_2$, product release rate constant $k_3$, and binding rate constant $k_{-3}$.

Rate constant experiments were set up like experiments performed with *trans*-HDV and *trans*-hammerhead ribozymes described previously[25,40,41] and are briefly described below.

$k_2$. The first-order rate constant was obtained from single-turnover experiments with an excess of various concentrations of ribozyme over substrate. The apparent rate constant ($k_{obs}$) was analyzed using denaturing PAGE and modeled with eq 2

$$k_{obs} = \frac{k_2[RZ]_{tot}}{K_M' + [RZ]_{tot}} \quad (2)$$



DOI: 10.1021/acs.biochem.7b00789
*Biochemistry* 2018, 57, 1440−1450

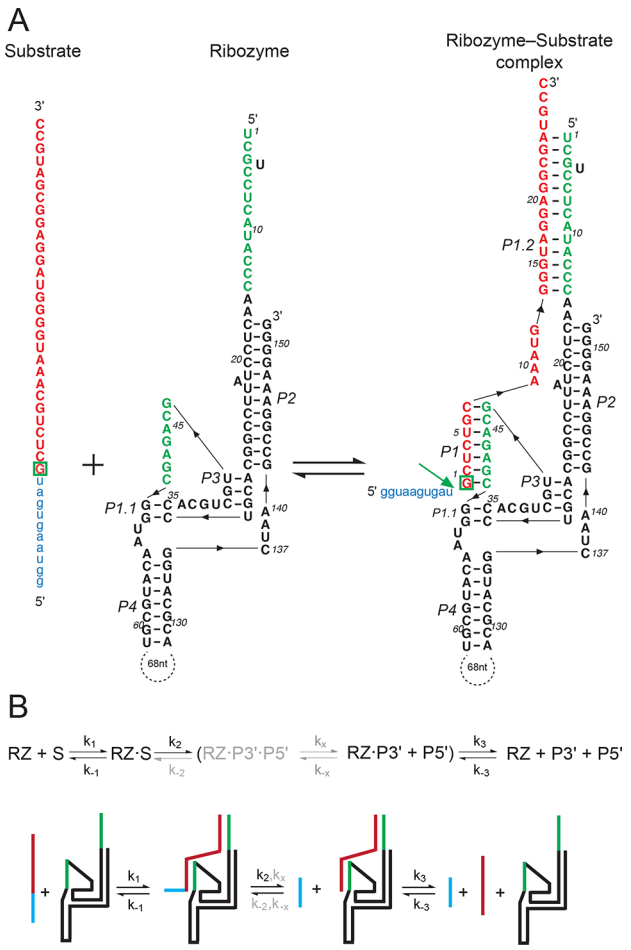


**Figure 1.** Secondary structure of *trans*-drz-Agam-2-1. (A) The blue lowercase letters on the substrate strand represent the leader sequence and the red uppercase letters the positions that bind the ribozyme, which is shown in green and black letters. The green box indicates the first nucleotide position, and the arrow indicates the cleavage site. Paired regions are designated with italicized P1–P4. The *trans*-cleaving ribozyme is derived from a self-cleaving sequence that is identical to the one shown here, except that *cis*-drz-Agam-2-1 is joined to a single RNA strand at the peripheral end of P1.2. (B) Minimal kinetic scheme of the *trans*-drz-Agam-2-1 ribozyme. The color scheme for the secondary structure is the same as in panel A. Gray color indicates the rate constants that were not determined in this study.

where $[RZ]_{tot}$ is the total ribozyme concentration and $K_M'$ is the modified Michaelis–Menten constant, derived from the titration of the enzyme (rather than the substrate).

*$k_1$ and $k_{-3}$.* The substrate association rate constant ($k_1$) was measured with varying concentrations of the ribozyme and analyzed with native PAGE. Low concentrations of excess ribozyme were incubated with $Mg^{2+}$-containing buffer, and in each case, the reaction was initiated by mixing with 1 nM 3′-labeled substrate. After each time period, the reaction was stopped by loading the sample onto a running gel (i.e., while the electric field was applied) to separate the ribozyme-bound substrates from the unbound fraction. Each binding kinetic rate constant was determined from the rate of the shift of the substrate to slower-migrating species and plotted against the ribozyme concentration. Association rate constants were modeled with eq 3 and extracted from the slope of the plot.

$$k_{obs} = k_{on}[RZ] + k_{off} \quad (3)$$

The rate constants for association of the ribozyme with the cleaved product were determined analogously using the purified cleaved 3′-product strand. The 3′-labeled cleaved product was incubated with various low concentrations of ribozyme (5–160 nM), and aliquots of the reaction were loaded directly on the native gel. Observed rate $k_{obs}$ was plotted as a function of ribozyme concentration.

*$k_{-1}$.* The substrate dissociation rate constant was measured by a pulse–chase experiment shown in Scheme 1.

**Scheme 1**

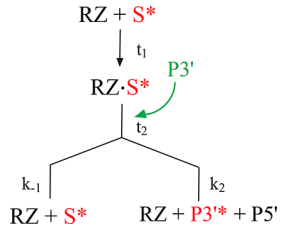


An excess of ribozyme (500 nM) was incubated with 1 nM 3′-labeled substrate for 30 s for the first time period, $t_1$, and then chased with 5 $\mu$M unlabeled 3′-product ([P3′] > 10[RZ]), which competes for the ribozyme base paring interactions with the substrate, for various times $t_2$ (from 10 s to 2 h), and then the reaction was quenched by EDTA loading buffer or the mixture loaded directly onto the running native gel at the end of each time point. The control reaction was quenched by EDTA loading buffer without chase for each $t_2$ (from 0 s to 2 h) or the mixture loaded directly onto the running native gel at the end of each time point. The rate of appearance of the free substrate was determined by measuring the intensity of the band corresponding to the free substrate as a fraction of total labeled species over time.

$$k_{obs} = k_2 + k_{-1} \quad (4)$$

*$k_3$.* The cleaved product dissociation rate constant was also measured by a pulse–chase experiment (Scheme 2).

**Scheme 2**

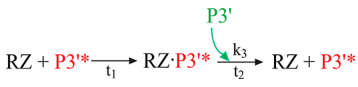


Ribozyme (100 nM) was incubated with 1 nM 3′-labeled cleaved product for 1 h ($t_1$), followed by a chase with 5 $\mu$M unlabeled product ([P] = 50[RZ]) for various times $t_2$ (from 30 s to 2 days). Sample aliquots were loaded into the running native gel at each time point. The rate of disappearance of the ribozyme–product complex was plotted against $t_2$ and fit to the fraction intact equation (eq 1).

*$K_d$.* The upper limit of the equilibrium dissociation constant was obtained by native PAGE of the complexes. A trace amount of 3′-labeled substrate or cleaved product was incubated with various ribozyme concentrations for 1 h, and then the samples were resolved via nondenaturing PAGE. The fraction of the bound sample was plotted against the concentration of ribozymes and modeled with the specific binding equation (eq 5)

$$\text{specific binding} = \frac{[RZ]^n B_{max}}{K_d^{\,n} + [RZ]^n} \quad (5)$$



DOI: 10.1021/acs.biochem.7b00789
*Biochemistry* 2018, 57, 1440–1450

where [RZ] is the ribozyme concentration, $B_{max}$ is the calculated maximum binding (typically, the binding fraction at saturation), and $n$ is the Hill coefficient. The measurement represents only the upper limit of the true dissociation constant in experiments with large dissociation rate constants, as was the case for the longest cleaved product.

**Bioinformatics. RNArobo/RNAbob Descriptor of the HDV-like *trans*-Ribozyme Core.** The following descriptor was used to search for sequences potentially capable of folding into the secondary structure assumed by HDV-like ribozymes lacking the 5′-strand of the P1 helix. The searched structure consists of elements that make up the secondary structure and the catalytic core of a *trans*-Agam-2 family of ribozymes. The 25 nts upstream of the ribozyme core are included in the descriptor to allow for (1) testing for folding of the upstream sequence to form a canonical P1 helix of the HDV-like ribozymes, thus forming a putative self-cleaving sequence, and (2) identifying sequences that can potentially form a P1.2 helix in *trans* with another RNA, revealing potential stable ribozyme−substrate pairs for *trans* scission. In the descriptor, h2, r3, and h4 correspond to helices (paired regions) P2, P3, and P4 of the HDV-like ribozymes, respectively (Chart 1).

**Chart 1**

```
# HDV−like ribozyme core with additional 25 nts at the 5′ end

s1 h2 r3 s2 r3' s3 s4 h4 s5 h4' s6 h2' s7

s1 0 NNNNNNNN[17]

h2 0:0 NNNNNN:NNNNNN

r3 0:0 NNN:NNN TGCA

s2 0 TYCHCG*N

s3 0 *NNNNNY

s4 0 GN*****

h4 0:0 NNNN****:****NNNN

s5 0 N[100]

s6 0 *CNRA*

s7 0 NNNNNNNNNN
```

RNArobo[42,43] was used to search the genome of the African mosquito *A. gambiae* for sequences that satisfy the sequence and secondary structure requirements specified by the descriptor. All sequences were tested for their potential to fold into self-cleaving ribozymes by their predicated ability to assume the pseudoknot structure of HDV-like ribozymes that includes a P1 helix with a guanosine at the 5′-terminus using the program DotKnot.[44] Sequences that did not fold into apparent self-cleaving ribozymes were further tested for predicted folding into the correct secondary structure of the *trans*-cleaving ribozyme core using the Vienna RNAfold server.[45] Assuming that the correctly predicted folds are more likely to act as *trans*-cleaving ribozymes, sequences predicted to form P2, P3, and P4 helices were ranked by the predicted overall stability of the helices. To better compare sequences of highly variable lengths of the predicted P4 regions (9−117 nts long, defined by h4 and s5 in the descriptor), we divided the predicted energy of formation of the P4−L4 domain by its length and reordered the sequences based on the stability of the P2, P3, and normalized P4−L4 regions.

We searched the *A. gambiae*-expressed sequence tags (EST) database to look for potential ribozyme substrates, because our previous search for self-cleaving ribozymes revealed many examples of self-cleaved constructs mapping to the 5′-termini of expressed sequences[9,14,20,46] and because they provide direct evidence of expression. We designed a descriptor for potential substrates of the *trans*-cleaving ribozymes identified above. The descriptor consisted of a 7 nt sequence that could perfectly base pair with the putative ribozyme's P1′ sequence, and any EST sequence that matched this requirement within the first 20 nts was subjected to further filtering. We considered the first 20 nts of the ESTs, and not just the first 7 nts, because some of the ESTs that matched the self-cleaved ribozymes identified in our previous work contained additional 5′-sequences that originated from the mapping experiments, such as 5′-templates used in rapid amplification of cDNA ends (RACE) or pieces of cloning vectors.[9,14,20,46] We included additional 20 nts downstream of the P1-matching sequence, and the putative substrate strand was tested for predicted formation of a stable interaction with the first 25 nts of the 5′-sequence of the putative ribozyme (s1 sequence in the structure descriptor above) using the RNAcofold program.[45] The putative substrates were ranked according to the predicted structure of the P1 and J1/2 domains (correct P1 helix and overall predicted stability of the P1.2 interaction), their frequency in the EST database, the number of copies within the genome, and gene proximity. Several of the top candidates were tested for *in vitro* activity.

## RESULTS

**Construction of *trans*-Cleaving Ribozymes from *cis*-Cleaving Forms.** HDV ribozymes can be converted into *trans*-acting forms by bisecting the J1/2 or L4 region.[24,47] Although splitting the ribozymes in the L4 loop results in more extensive base pairing, which increases binding specificity and allows incorporation of modified nucleotides into the active site,[48] the J1/2-bisected molecule preserves the ribozyme core and recognizes a target (substrate) strand exclusive of any catalytic components. The design of J1/2-split molecules has previously led to ribozymes that could cleave target RNAs *in vitro* and *in vivo*.[25−27,41,47,49−55]

Drz-Agam-2-1 (GenBank entry BK006881) was the first genomic HDV-like ribozyme discovered to contain a long J1/2 insertion that forms an additional helix (P1.2),[14] which greatly stabilizes the activated form of the ribozyme, leading to efficient catalysis.[23] Because a preorganized P1.2 helix apparently lowers a conformational barrier related to a rate-limiting conformational change in the ribozyme,[23] we decided to test the ribozyme for RNA scission in *trans*. The *trans*-ribozyme and its corresponding substrate were constructed by bisecting the P1.2 stem−loop structure of drz-Agam-2-1 at the distal end, creating a substrate strand consisting of the leader sequence (upstream of the cleavage site) and the 5′-strand of the P1 and P1.2 helices, and a ribozyme strand consisting of the catalytic core with the P1 and P1.2 sequences recognizing the substrate strand (Figure 1A). Similar constructs have previously been engineered on the basis of HDV ribozymes, but their kinetic parameters were not studied in depth.[51,56,57]

**Minimal Kinetic Mechanism.** Intermolecular HDV-like ribozyme scission involves the assembly of the ribozyme−substrate complex from the catalytic core (the ribozyme) and



DOI: 10.1021/acs.biochem.7b00789
*Biochemistry* 2018, 57, 1440−1450

substrate strand, phosphodiester bond scission, and release of the product from the ribozyme−product complex (Figure 1). Except for the reverse of the catalytic cleavage step (ligation) and the binding of the 5′-product (the leader sequence), which were not tested because the 5′-product is thought to have a vanishingly low affinity for the HDV ribozymes,[25] all other major steps have forward and reverse reaction rate constants that can be detected by straightforward biochemical analysis.

The pre-steady-state catalytic rate constant ($k_2$) for intermolecular cleavage was measured under single-turnover conditions, when the ribozyme is in excess over the substrate ([RZ]/[S] > 5). The observed rate constants were plotted against ribozyme concentration and fit with eq 2. $K_M'$ and $k_2$ were calculated to be 4020 nM and 1.7 $min^{-1}$, respectively (Figure 2), which yield a second-order rate constant ($k_2/K_M'$)

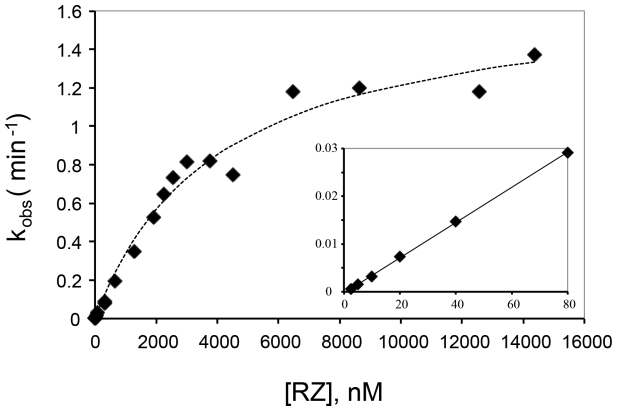


**Figure 2.** Single-turnover cleavage by the *trans*-drz-Agam-2-1 ribozyme. The reaction was performed at 37 °C with 1 mM $Mg^{2+}$. The rate constant corresponding to the chemical step ($k_2$) at saturating ribozyme concentrations is 1.7 $min^{-1}$, and the ribozyme concentration at half-maximum activity ($K_M'$) is 4020 nM. The inset shows the second-order rate constant ($k_2/K_M' = 4 \times 10^5$ $M^{-1}$ $min^{-1}$) as the slope of $k_{obs}$ at low ribozyme concentrations.

of $4.3 \times 10^5$ $M^{-1}$ $min^{-1}$. This value agrees with the slope of $4 \times 10^5$ $M^{-1}$ $min^{-1}$ in the $k_{obs}$ versus ribozyme plot at low concentrations in the inset of Figure 2.

The two paired regions of interaction between the substrate and the ribozyme provided enough stability that the *trans*-cleaving complex could be directly detected by an electrophoretic mobility shift assay (EMSA) using a nondenaturing (native) PAGE, and we used this method to measure the substrate association rate constant (Figure 3A). According to eq 3, the slope of the graph ($8 \times 10^5$ $M^{-1}$ $min^{-1}$) represents the association rate constant of the substrate (Figure 3B).

To measure the substrate dissociation rate constant, a pulse−chase experiment was used, as outlined in Scheme 1 and calculated using eq 4, where $k_2$ was the control reaction rate constant and $k_{-1}$ was determined to be 0.018 $min^{-1}$ (Figure S1). When $k_{-1}$ (0.018 $min^{-1}$) ≪ $k_2$ (1.7 $min^{-1}$), the second-order rate constant ($k_2/K_M'$) is reduced to the substrate binding rate constant [$k_2/K_M' = k_2k_1/(k_2 + k_{-1}) \sim k_1$]. This is confirmed by the experimental $k_1$ value of $8 \times 10^5$ $M^{-1}$ $min^{-1}$, which is similar to the calculated $k_2/K_M'$ of $4.3 \times 10^5$ $M^{-1}$ $min^{-1}$ described above.

Equilibrium dissociation constant $K_d$ of the substrate was estimated using an EMSA (Figure S2). The $K_d$ for the substrate was calculated to be 27 ± 5 nM [average and average deviation of three experiments (Figure S2C)] and likely represents the

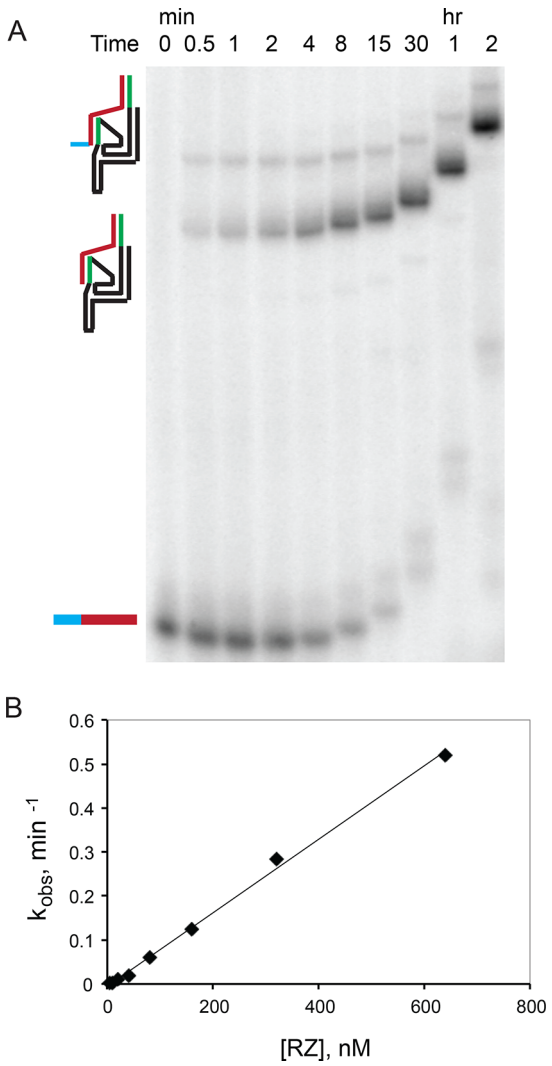


**Figure 3.** Measurement of the substrate association rate constant ($k_1$). (A) Native PAGE of the substrate binding kinetics, revealing a stable ribozyme−substrate complex unique to HDV-like ribozymes with a P1.2 peripheral domain. The secondary structure color scheme is the same as that used for Figure 1, indicating the bands corresponding to the free substrate (bottom band, blue−red), its complex with the ribozyme, and the product complex (top bands). (B) The substrate association rate constant was determined to be $8 \times 10^5$ $M^{-1}$ $min^{-1}$ from the slope of the observed rate constant vs ribozyme concentration.

upper limit of the true dissociation constant, given that the incubation time was only slightly longer than the half-life of the complex, as calculated from $k_{-1}$ (0.018 $min^{-1}$ = 1.08 $h^{-1}$; $t_{1/2} \sim$ 0.6 h). The Hill constant was calculated to be 1.6 ± 0.08.

The equilibrium binding constant of the substrate was also calculated from the ratio of dissociation and association rate constants (0.018 $min^{-1}$ and $8 \times 10^5$ $M^{-1}$ $min^{-1}$, respectively) and reveals a value of 22.5 nM, similar to the lower range of the values measured by the direct binding experiment (27 ± 5 nM). Interestingly, this value is ∼180 times lower than the $K_M'$ of the ribozyme with the same substrate (4020 nM) and suggests that a substantial activation barrier separates the bound complex from the catalytically competent complex, as we previously suggested for the *cis* form of this ribozyme.[23]

The release rate constant ($k_3$) of the cleaved product was calculated to be $3.9 \times 10^{-5}$ $min^{-1}$ = 0.056 $day^{-1}$ (Figure S3).



DOI: 10.1021/acs.biochem.7b00789
*Biochemistry* 2018, 57, 1440−1450

This rate corresponds to a half-life of ~12 days, which is similar to the half-life of $^{32}$P (14.3 days); however, because the measurement is calculated from the fraction liberated from the complex, the rate constant is not affected by $^{32}$P decay. In agreement with the very slow product release rate, but in contrast to the case of the *trans*-antigenomic HDV ribozyme,[25] we observed no multiple-turnover activity for *trans*-drz-Agam-2-1.

The product binding rate constant was obtained in a manner similar to that of the substrate (Figure S4). Fitting the data to eq 3 revealed a slope of $8 \times 10^5$ $M^{-1}$ $min^{-1}$, which represents product binding rate constant $k_{-3}$ (Figure S4B). The rate constant is identical to the binding rate constant of the substrate (see above).

Like substrate dissociation constant $K_D(S)$, equilibrium dissociation constant $K_D(P)$ of the cleaved product was analyzed with an EMSA after incubation of the ribozyme with the cleaved product for 1 h (Figure S5). The fraction bound was plotted against the concentration of ribozyme and fit with the specific binding equation (eq 5). The $K_D$ for the cleaved product was calculated to be 11.5 ± 1.5 nM (Figure S5B; $n$ = 2) with a Hill coefficient of 2.4 ± 0.1. However, because of the very slow product release rate, these data represent the upper limit, not equilibrium, of the dissociation constant. The half-life of the product complex is 12 days, which means the reaction mixture must be incubated for several weeks to reach equilibrium; therefore, the EMSA-based analysis represents only an upper estimate of the true $K_D$. Indeed, estimation of $K_D(P)$ from the association and dissociation rate constants reveals a value of ($3.9 \times 10^{-5}$ $min^{-1}$/$8 \times 10^5$ $M^{-1}$ $min^{-1}$) ~ 50 pM, indicating that the EMSA-based measurement of the $K_D(P)$ equilibrium greatly overestimated the true value. The $K_D(P)$ is also ~460 times smaller than the $K_D(S)$, confirming a previously published result proposing that the substrate destabilizes the ground-state energy to activate the HDV ribozymes;[58] however, in the case of the Agam-2-1 ribozyme, the difference in $K_D$ values is substantially larger.

**Substrates with Shorter Recognition Sequences.** To compare the activity of the *trans*-Agam-2-1 ribozyme with that of the HDV ribozymes, we tested it with a short substrate lacking the J1/2 region and forming a complex with the ribozyme through only 7 bp of the P1 helix. This substrate exhibited undetectable $k_{obs}$ under 1 mM $Mg^{2+}$ conditions (1 nM substrate and 900 nM ribozyme) and a detectable but very small $k_{obs}$ of 0.01 $h^{-1}$ when the $Mg^{2+}$ concentration was increased to 10 mM (Figure S6). These data supported the previous observation that the $Mg^{2+}$ requirement becomes stronger in ribozymes lacking the J1/2 domain[23,59] and confirm our previous results with the Agam-2-1 ribozyme, showing that the stable J1/2 structure increases the cleavage rate.[23] No direct binding of either the 7 bp substrate or its cleaved product was detected. On the other hand, when we tested an intermediate-length RNA strand that formed 7 bp in the P1 and (4 or) 5 bp in the P1.2 regions (see the Supporting Information for the truncated sequence and predicted interaction with the ribozyme), formation of the complex between the cleaved substrate and the ribozyme was observed using native PAGE. At 14 nM, the $K_d$ of this RNA, tested at 100 pM and incubated with the *trans*-Agam-2-1 ribozyme for 4 days, was weaker than that of the full-length product ($K_D$ ~ 50 pM). These results confirm that *trans*-Agam-2-1 forms stable complexes with substrates that span both P1 and P1.2 helices and cleaves these substrates efficiently, and the strength of the interaction depends on the number of base pairs between the two RNA strands. The kinetic parameters are summarized in Figure 4 and Table 1.

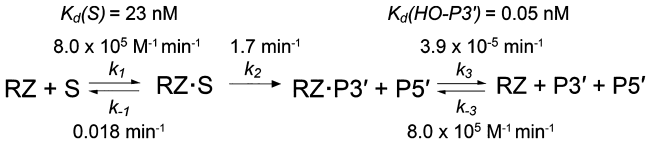


**Figure 4.** Summary of the kinetic parameters of the *trans*-drz-Agam-2-1 ribozyme. The equilibrium dissociation constants were calculated from the on- and off-rate constants for the substrate and product.

**Table 1. Comparison of the Kinetic Parameters of *trans*-Cleaving drz-Agam-2-1 and Antigenomic HDV Ribozymes**

| | *trans*-Agam-2-1 | *trans*-aHDV[a,b] |
|---|---|---|
| $k_1$ | $8.0 \times 10^5$ $M^{-1}$ $min^{-1}$ | $2.1 \times 10^7$ $M^{-1}$ $min^{-1}$[a] |
| $k_{-1}$ | 0.018 $min^{-1}$ | 1.4 $min^{-1}$[a] |
| $K_M'$ | 4020 nM | 110 nM[a] |
| | | 18, 17 nM[§] |
| $k_2$ | 1.7 $min^{-1}$ | 0.91 $min^{-1}$[a] |
| | | 0.34 $min^{-1}$[b] |
| $k_3$ | $3.9 \times 10^{-5}$ $min^{-1}$ | $6.0 \times 10^{-3}$ $min^{-1}$[a] |
| $k_{-3}$ | $8.0 \times 10^5$ $M^{-1}$ $min^{-1}$ | $2.3 \times 10^6$ $M^{-1}$ $min^{-1}$[a] |
| $K_d(S)$ | 27 nM | 58 nM[a] |
| | | 32 nM[b] |
| $K_d(P)$ | 0.050 nM | 2.5 nM[a] |
| $K_d(P^{NN})$ | 0.063 aM[c] | 9.3 nM (WT)[a–c] |
| | | 3.9 nM[b,c] |
| $K_d(P_{mid})$ | 14 nM | |
| $K_d(P^{NN})$ | 28 pM[c] | |
| $k_2/K_M'$ | $4.3 \times 10^5$ $M^{-1}$ $min^{-1}$ | $8.3 \times 10^6$ $M^{-1}$ $min^{-1}$[a] |
| | | $1.9 \times 10^7$ $M^{-1}$ $min^{-1}$[b] |
| | | $0.8 \times 10^7$ $M^{-1}$ $min^{-1}$[b] |

[a]Data for the *trans*-cleaving antigenomic HDV ribozyme (aHDV) collected in 40 mM Tris-HCl (pH 8.0) and 10 mM $MgCl_2$ at 37 °C.[25] [b]Data for two *trans*-aHDV ribozymes with distinct P1 sequences measured in 50 mM Tris-HCl (pH 7.5) and 10 mM $MgCl_2$ at 37 °C.[68] [c]$K_d(P^{NN})$ refers to the dissociation constant calculated on the basis of a nearest-neighbor thermodynamic model using RNAcofold.[75] The calculated free energies and predicted base pairs of the RNA heterodimers are presented in the Supporting Information.

The extension of the HDV-like ribozyme into the P1.2 region allows recognition of the substrate strand through a longer sequence, which is additionally reflected in the specificity of the *trans* scission. *trans*-cleaving HDV ribozymes can recognize their substrates only through 7 bp and can therefore specify only 1 of ~4000 sequences, assuming that the first nucleotide after the cleavage site has to be a guanosine and the other six are specified by the P1 sequence on the ribozyme strand ($4^6$ = 4096). On the other hand, a substrate strand that spans the P1 and P1.2 helices can be recognized through additional base pairs, increasing the specificity by ~$4^N$ times, where $N$ is the number of P1.2 base pairs. For the long substrate presented here (Figure 1A), the overall specificity is almost $10^{11}$ (for the 6 and 12 bp of P1 and P1.2, respectively, $4^6 \times 4^{12} = 6.9 \times 10^{10}$), much greater than the theoretical sequence diversity of any genome (e.g., the length of the haploid human genome is ~$3 \times 10^9$ bp, and its theoretical sequence diversity is ~$6 \times 10^9$ when the genome is transcribed in both directions). This result implies that the Agam-2-1-like *trans*-cleaving


DOI: 10.1021/acs.biochem.7b00789
Biochemistry 2018, 57, 1440–1450

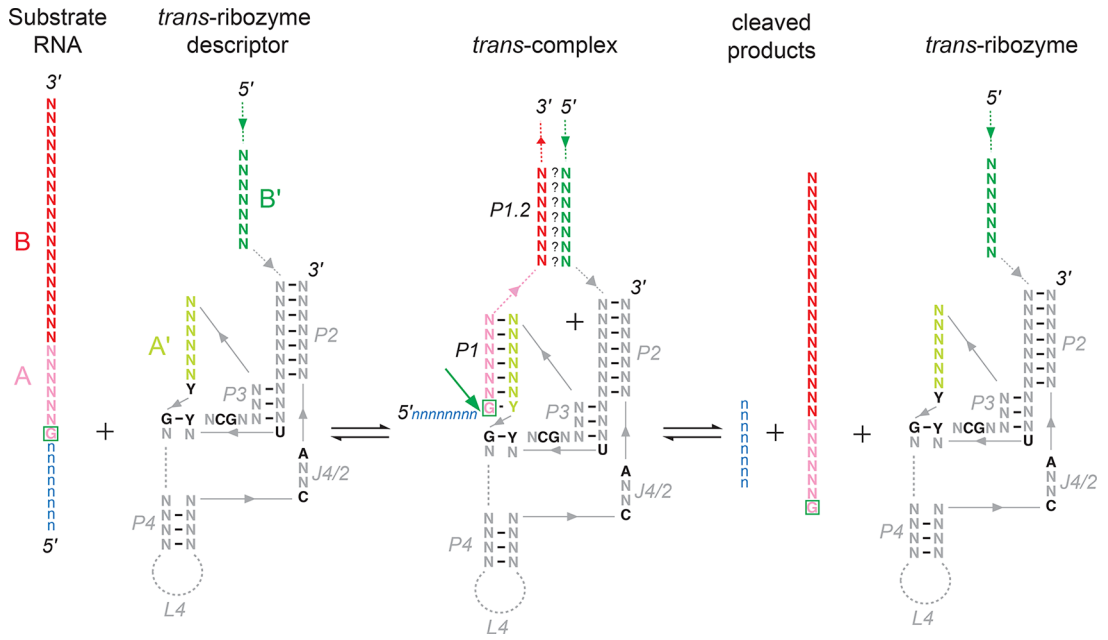


**Figure 5.** Structure-based search for genomic *trans*-cleaving ribozymes. A descriptor of the secondary structure of the catalytic strand of a generic HDV-like ribozyme was used to find sequences capable of assuming the fold of a *trans*-ribozyme. Sequences with computationally validated secondary structures were used as templates (in regions A′ and B′) for sequence-based searches through the *A. gambiae* EST database for RNAs with perfectly matching A segments and at least partially matching B segments. The A and B strands were computationally validated to form correct P1 and P1.2 helices, while the rest of the secondary structure of the ribozyme was maintained (*trans* complex). Top candidates were tested for *trans* scission *in vitro* by monitoring product formation.

ribozymes could have evolved (or be engineered[60]) to cut unique target RNAs even in organisms with highly complex transcriptomes. Motivated by this hypothesis, we designed a bioinformatics approach to search for potential ribozyme−substrate pairs in the *A. gambiae* genome.

***trans*-Acting Ribozyme and Potential Substrates Revealed by Structure-Based Bioinformatics in the *A. gambiae* Genome.** We chose to search for *trans*-acting HDV-like ribozymes in the genome of *A. gambiae* because of its complete genomic database, extensive expressed sequence tags (EST) database, material availability, abundance of self-cleaving ribozymes, and our previous analyses of *cis*-drz-Agam-2-1 constructs.[13,14,23] On the basis of the design of the *trans*-acting Agam-2-1 (Figure 1A), we designed a descriptor for the structure-based search consisting of the catalytic core of the *trans*-ribozyme, which contained one strand of P1.2 and P1 each. This core ribozyme does not self-cleave but is capable of forming interactions with another RNA through base pairing with complementary P1.2 and P1 sequences (Figure 5). Self-cleaving HDV-like ribozymes served as controls for the structure-based search, because we expected it to yield all HDV-like catalytic cores, including the six previously described families of *A. gambiae cis*-cleaving ribozymes.[37,53,56]

We applied a descriptor for a generic HDV-like ribozyme core to perform the initial search and filtering, yielding ∼50 putative ribozymes. We then chose the most stable ribozymes lacking any predicted ability to fold into a *cis*-cleaving ribozyme, which narrowed the yield to ∼40 sequences, of which only five were putative *trans*-cleaving ribozymes with the predicted correct P4−L4 domain (the predicted structure was required to form a helix between the 5′- and 3′-termini of the domain). Finally, we used the ribozyme with the most stable predicted secondary structure to search for potential substrates (see Materials and Methods for details of the approach). This sequence, the *trans*-ribozyme-69, was selected for *in vitro* analysis (Figure 6A). A substrate search revealed a sequence in chromosome 2L (substrate-14), which was chosen because it appears twice in the EST database and maps to the first exon of a gene (Figure 6B). The putative cleavage site maps to the 10th nucleotide of the two ESTs, and the substrate forms 11 bp in the assembled P1.2 region, in addition to the 7 bp of the P1 helix. The *trans* cleavage rate was determined with a 3′-labeled substrate under single-turnover conditions, with the ribozyme preincubated with $Mg^{2+}$ to test for independent folding under physiological-like conditions. We initiated the *trans* scission by adding the substrate. The pseudo-first-order rate constant was measured to be 5.1 $h^{-1}$ ($t_{1/2}$ ∼ 6 min) at 10 mM $Mg^{2+}$ and 37 °C (500 nM ribozyme and 2 nM substrate) (Figure 6C,D). This rate constant is similar to many rate constants of HDV-like self-cleaving ribozymes under similar experimental conditions.[13,14,19,20]

We also tested a second potential substrate of *trans*-ribozyme-69 [substrate-53 (Figure S7A)], in which the cleavage site maps to the 5′-terminus of EST BM622397.1 and corresponds to the first position in the first exon of a lipoprotein N-terminal domain of a vitellogenin-like protein gene on chromosome 3R (Figure S7B). This RNA forms 12 bp with *trans*-ribozyme-69 in the J1/2 region; however, its scission was significantly slower, with a pseudo-first-order rate constant of only 0.16 $h^{-1}$ at 10 mM $Mg^{2+}$ and 37 °C (Figure S7C,D). Nonetheless, these examples demonstrate that our bioinformatics strategy is successful in revealing novel genomic *trans*-cleaving ribozymes and their putative substrates.

## ■ DISCUSSION

The widespread distribution of self-cleaving ribozymes throughout the genomes of bacteria and eukaryotes[2,9,10,12−14,61−67] led us to ask whether ribozymes that



DOI: 10.1021/acs.biochem.7b00789
*Biochemistry* 2018, 57, 1440−1450

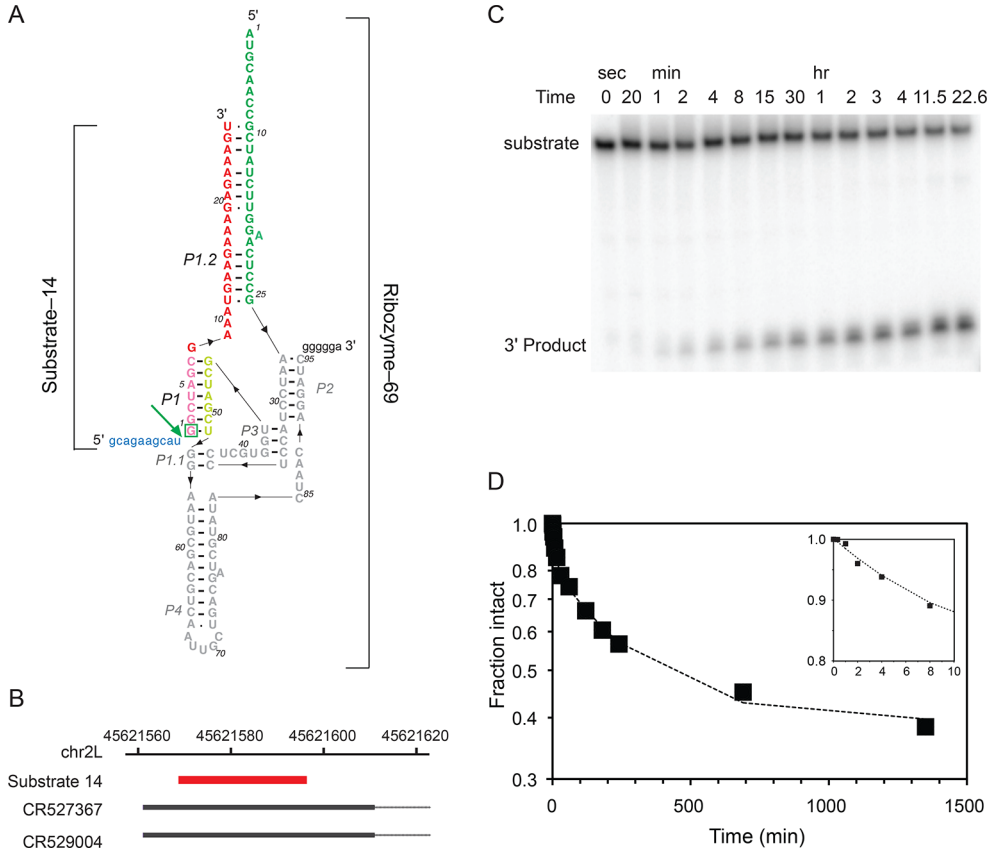


**Figure 6.** Activity of the *trans*-acting Agam-ribozyme-69 and substrate-14. (A) Predicted secondary structure of the complex consisting of the ribozyme (mapping to ChrU:21393977-21394076) and the substrate mapping near the 5′-termini of two ESTs (CR529004 and CR527367) corresponding to the λ crystallin-like gene in *A. gambiae*. (B) The color scheme is the same as in Figure 5. (C) Denaturing PAGE of the *trans* scission of body-labeled substrate-14 at 10 mM $Mg^{2+}$ and 37 °C. (D) Semilogarithmic graph of the *in vitro* cleavage activity of the *trans*-ribozyme. The inset shows the initial data points plotted on a linear graph.

cleave other RNAs in *trans* exist in nature. Mechanistically, a *trans*-cleaving ribozyme can arise by dividing a *cis*-ribozyme into two pieces that correspond to the catalytic domain and the substrate strand. The *trans*-HDV ribozyme was previously constructed to study the kinetics of cleavage[25,68] and for gene knockdown experiments;[27,49−51] however, the short 7 nt binding region for the *trans*-ribozyme substrate provided little utility for the construct, even though it was useful for defining the kinetic parameters of the HDV ribozymes. The long P1.2 insertion discovered in *A. gambiae* and other insect ribozymes[10,13,14] could serve for stronger target RNA recognition, if the domain was bisected to yield two RNAs, a ribozyme and a long substrate, and a similar approach has been proposed for engineering HDV ribozymes into more specific *trans* cleavers.[51,60] To evaluate the influence of the long target binding sequence, it is imperative that the kinetic parameters of such ribozymes be measured to assess the usefulness of these catalysts for cellular targeting and cleavage of single-stranded RNAs. We therefore set out to study the mechanism of cleavage by utilizing the intermolecular HDV-like ribozyme and its substrate derived from the drz-Agam-2-1 ribozyme.

We established the minimal kinetic scheme (Figure 1B), and the resulting rate and equilibrium constants are summarized in Figure 4 and Table 1. The data provide a view of *trans*-acting HDV-like ribozyme kinetics that was broader than that previously determined for J1/2-extended ribozymes, as well as a guideline for the discovery or engineering of *trans*-ribozymes. This study also afforded a more detailed view of the energetics of activation of HDV-like ribozymes.

Our kinetic measurements revealed that the Agam-2-1-derived ribozyme binds the full-length substrate with a high affinity that depends on the number of base pairs in both helices P1 and P1.2. The affinity of the substrate spanning both P1 and P1.2 is similar to that of short substrates (binding only through the 7 bp of the P1 helix), previously tested with antigenomic HDV (aHDV) ribozymes (Table 1).[25,68] This result, together with the unexpectedly high $K_M'$, suggests that the ribozyme-catalyzed cleavage includes an energetic penalty for binding substrates spanning both helical regions. This penalty is particularly manifest in the substantially lower $k_1$, the on-rate binding constant of the substrate, and agrees with a previously proposed model in which we suggested that HDV-like ribozymes have to overcome an energetic barrier related to activation of the ribozymes from a relaxed, precatalytic conformation to a catalytically competent form.[23]

Further evidence for this model is based on the measurement of the binding kinetics of the *trans*-cleaved products. Whereas the full-length *trans*-Agam-2-1 substrate binds with an affinity similar to that of RNA strands that are exclusively P1-interacting [$K_d$ values of 27 and 32−58 nM for the Agam and aHDV ribozymes, respectively (Table 1)], the cleavage product binds with a similar on-rate but its kinetics of release are substantially slower ($t_{1/2}$ ∼ 2 weeks; $K_d$ = 50 pM). Furthermore, the measured $K_d$ for the *trans*-Agam-2-1 product is much higher than would be expected from thermodynamic


DOI: 10.1021/acs.biochem.7b00789
*Biochemistry* 2018, 57, 1440−1450

calculations,[69] contrasting with the short product of the aHDV, which binds with an affinity similar to the predicted value [$K_d$(P) vs $K_d$($P^{NN}$) (Table 1)]. The release rate constants for the *trans*-Agam-2-1 substrate and product differ by ~500. The effect on the affinities can be partially attributed to the ground-state destabilization of the ribozyme by the substrate, as has previously been suggested for the aHDV ribozyme,[25,58] as well as the hammerhead ribozyme,[70] and self-splicing in the *Tetrahymena* group I intron.[71,72] In aHDV, the product binds the ribozymes ~25 times more strongly; therefore, if the activation by the substrate observed in the antigenomic HDV ribozyme accounts for ~25-fold of the Agam ribozyme difference, ~20-fold remains to account for the conformational activation of the ribozyme. Thus, in the case of the extended HDV-like ribozymes, the energetic penalty can be divided approximately evenly between formation of the catalytically competent state and substrate-activated catalysis.

The extremely low rate constant ($3.9 \times 10^{-5}$ $min^{-1}$) of 3′-product release is related to the exceptional stability of the ribozyme−product complex but is also the reason why there was no multiple-turnover activity observed for the *trans*-Agam-2-1 ribozyme. This result demonstrates the trade-off between the increased substrate specificity and the low rate of turnover in ribozymes derived from self-cleaving sequences and implies that an at least stoichiometric amount of the *trans*-ribozyme is needed for the application of target RNA cleavage with long *trans*-acting ribozymes. Alternatively, a mechanism for accelerated dissociation of the product complex, e.g., by RNA helicases, would have to be involved to increase the rate of *trans*-scission turnover. Nonetheless, the extended *trans*-cleaving ribozymes show high substrate affinity and robust activity to motivate a search for genomic *trans*-cleaving ribozymes.

On the basis of our earlier implementation of structure-based bioinformatics in the discovery of genomic self-cleaving ribozymes,[14,73,74] we devised a strategy to search through the genome of *A. gambiae* for sequences capable of forming putative *trans*-cleaving HDV-like ribozymes and coupled the results to a search for their potential substrates among expressed sequences. We chose to test the most stable of the predicted *trans*-HDV-like ribozyme (*trans*-Agam-69) and two of its putative substrates, both of which map to the 5′-termini of *A. gambiae* ESTs.

*trans*-Agam-69 substrate-53 maps to the first nucleotide of the first exon in the EST, which indicates that there may be a cleaving process operated by the *trans*-ribozyme. The other substrate (substrate-14), mapped to the 10th nucleotide of the first exon, also supports the putative role of a *trans*-acing ribozyme. Both substrates are cleaved efficiently by the ribozyme *in vitro* (Figure 6 and Figure S7), confirming the feasibility of the bioinformatics approach for the discovery of ribozyme−substrate pairs. *trans*-Agam-69 maps to several introns of predicted genes, suggesting that it is expressed and can therefore be available for *trans* scission *in vivo*. Furthermore, like the *A. gambiae cis*-cleaving ribozymes,[13] this sequence may be associated with a transposable element because it is present in the genome in several copies and in most instances a sequence similar to the retrotransposon Gypsy maps downstream of the ribozyme. *trans*-Agam-69 may therefore be a remnant of a self-cleaving ribozyme that was incompletely copied during retrotransposition and may represent a general mechanism of conversion of self-cleaving ribozymes to *trans* cleavers. Furthermore, the large abundance of self-cleaving ribozymes and their truncated variants in *A. gambiae* prompted us to look for potential ribozyme−substrate pairs in which the ribozyme was derived from a known self-cleaving sequence.

When we searched the *A. gambiae* genome for remnants of known *cis*-cleaving ribozymes, we found multiple instances of both drz-Agam-2-1 and -2-2 with weak P1.2 helices and missing 5′-strands. We searched the EST database for a potential substrate of one of these putative *trans*-Agam-2 ribozymes and found a sequence mapping to the 5′-terminus of mRNAs that encode alipoprotein D-like protein and are capable of forming an active complex with the *trans*-ribozyme (Figure S8). This example thus provides a mechanism for the emergence of *trans*-cleaving ribozymes from self-cleaving ones via incomplete copying of the RNA template during retrotransposition, leading to truncated versions of the self-cleaving ribozymes that map to the 5′-termini of these mobile genetic elements. Although we do not prove the *in vivo* activity of these ribozymes as *trans*-cleaving catalytic RNAs, we show that our method can uncover putative genomic ribozyme−substrate pairs and through them potential new modes of endogenous gene expression regulation.

## ■ ASSOCIATED CONTENT

### Supporting Information

The Supporting Information is available free of charge on the ACS Publications website at DOI: 10.1021/acs.biochem.7b00789.

Figures S1−S8 and DNA sequences (PDF)

## ■ AUTHOR INFORMATION


### Corresponding Author

*E-mail: aluptak@uci.edu.

### ORCID

Andrej Lupták: 0000-0002-0632-5442

### Present Address

‖C.-H.T.W.: ResearchDX, Irvine, CA 92618.



### Funding

This work was supported by the Pew Charitable Trusts (to A.L. through the Pew Scholars in Biomedical Sciences Program), the National Institutes of Health (R01GM094929), and the National Science Foundation (MCB 1330606). This work was made possible through the support of a grant from the John Templeton Foundation.


### Notes

The authors declare no competing financial interest.

## ■ ACKNOWLEDGMENTS


The authors thank members of the Lupták lab for helpful discussion and A. James for *A. gambiae* DNA.


## ■ REFERENCES


(1) Jimenez, R. M., Polanco, J. A., and Luptak, A. (2015) Chemistry and Biology of Self-Cleaving Ribozymes. *Trends Biochem. Sci. 40*, 648−661.

(2) Weinberg, Z., Kim, P. B., Chen, T. H., Li, S., Harris, K. A., Lunse, C. E., and Breaker, R. R. (2015) New classes of self-cleaving ribozymes revealed by comparative genomics analysis. *Nat. Chem. Biol. 11*, 606−610.

(3) Rizzetto, M., Canese, M. G., Arico, S., Crivelli, O., Trepo, C., Bonino, F., and Verme, G. (1977) Immunofluorescence detection of new antigen-antibody system (delta/anti- delta) associated to hepatitis B virus in liver and in serum of HBsAg carriers. *Gut 18*, 997−1003.




DOI: 10.1021/acs.biochem.7b00789
*Biochemistry* 2018, 57, 1440−1450

(4) Wu, H. N., Lin, Y. J., Lin, F. P., Makino, S., Chang, M. F., and Lai, M. M. (1989) Human hepatitis delta virus RNA subfragments contain an autocleavage activity. *Proc. Natl. Acad. Sci. U. S. A. 86*, 1831−1835.
(5) Sharmeen, L., Kuo, M. Y., Dinter-Gottlieb, G., and Taylor, J. (1988) Antigenomic RNA of human hepatitis delta virus can undergo self-cleavage. *J. Virol. 62*, 2674−2679.
(6) Kuo, M. Y., Sharmeen, L., Dinter-Gottlieb, G., and Taylor, J. (1988) Characterization of self-cleaving RNA sequences on the genome and antigenome of human hepatitis delta virus. *J. Virol. 62*, 4439−4444.
(7) Perrotta, A. T., and Been, M. D. (1991) A pseudoknot-like structure required for efficient self-cleavage of hepatitis delta virus RNA. *Nature 350*, 434−436.
(8) Wadkins, T. S., Perrotta, A. T., Ferre-D'Amare, A. R., Doudna, J. A., and Been, M. D. (1999) A nested double pseudoknot is required for self-cleavage activity of both the genomic and antigenomic hepatitis delta virus ribozymes. *RNA 5*, 720−727.
(9) Salehi-Ashtiani, K., Lupták, A., Litovchick, A., and Szostak, J. W. (2006) A genomewide search for ribozymes reveals an HDV-like sequence in the human CPEB3 gene. *Science 313*, 1788−1792.
(10) Eickbush, D. G., and Eickbush, T. H. (2010) R2 retrotransposons encode a self-cleaving ribozyme for processing from an rRNA cotranscript. *Mol. Cell. Biol. 30*, 3142−3150.
(11) Sanchez-Luque, F., Lopez, M. C., Macias, F., Alonso, C., and Thomas, M. C. (2012) Pr77 and L1TcRz: A dual system within the 5′-end of L1Tc retrotransposon, internal promoter and HDV-like ribozyme. *Mobile genetic elements 2*, 1−7.
(12) Sanchez-Luque, F. J., Lopez, M. C., Macias, F., Alonso, C., and Thomas, M. C. (2011) Identification of an hepatitis delta virus-like ribozyme at the mRNA 5′-end of the L1Tc retrotransposon from Trypanosoma cruzi. *Nucleic Acids Res. 39*, 8065−8077.
(13) Ruminski, D. J., Webb, C. H., Riccitelli, N. J., and Lupták, A. (2011) Processing and Translation Initiation of Non-long Terminal Repeat Retrotransposons by Hepatitis Delta Virus (HDV)-like Self-cleaving Ribozymes. *J. Biol. Chem. 286*, 41286−41295.
(14) Webb, C. H., Riccitelli, N. J., Ruminski, D. J., and Lupták, A. (2009) Widespread occurrence of self-cleaving ribozymes. *Science 326*, 953.
(15) Ferre-D'Amare, A. R., Zhou, K., and Doudna, J. A. (1998) Crystal structure of a hepatitis delta virus ribozyme. *Nature 395*, 567−574.
(16) Ke, A., Zhou, K., Ding, F., Cate, J. H., and Doudna, J. A. (2004) A conformational switch controls hepatitis delta virus ribozyme catalysis. *Nature 429*, 201−205.
(17) Chen, J. H., Yajima, R., Chadalavada, D. M., Chase, E., Bevilacqua, P. C., and Golden, B. L. (2010) A 1.9 A crystal structure of the HDV ribozyme precleavage suggests both Lewis acid and general acid mechanisms contribute to phosphodiester cleavage. *Biochemistry 49*, 6508−6518.
(18) Perrotta, A. T., and Been, M. D. (1990) The self-cleaving domain from the genomic RNA of hepatitis delta virus: sequence requirements and the effects of denaturant. *Nucleic Acids Res. 18*, 6821−6827.
(19) Riccitelli, N. J., Delwart, E., and Luptak, A. (2014) Identification of minimal HDV-like ribozymes with unique divalent metal ion dependence in the human microbiome. *Biochemistry 53*, 1616−1626.
(20) Webb, C. H., and Lupták, A. (2011) HDV-like self-cleaving ribozymes. *RNA Biol. 8*, 719−727.
(21) Been, M. D., Perrotta, A. T., and Rosenstein, S. P. (1992) Secondary structure of the self-cleaving RNA of hepatitis delta virus: applications to catalytic RNA design. *Biochemistry 31*, 11843−11852.
(22) Thill, G., Vasseur, M., and Tanner, N. K. (1993) Structural and sequence elements required for the self-cleaving activity of the hepatitis delta virus ribozyme. *Biochemistry 32*, 4254−4262.
(23) Webb, C. H., Nguyen, D., Myszka, M., and Luptak, A. (2016) Topological constraints of structural elements in regulation of catalytic activity in HDV-like self-cleaving ribozymes. *Sci. Rep. 6*, 28179.
(24) Branch, A. D., and Robertson, H. D. (1991) Efficient trans cleavage and a common structural motif for the ribozymes of the human hepatitis delta agent. *Proc. Natl. Acad. Sci. U. S. A. 88*, 10163−10167.
(25) Shih, I., and Been, M. D. (2000) Kinetic scheme for intermolecular RNA cleavage by a ribozyme derived from hepatitis delta virus RNA. *Biochemistry 39*, 9055−9066.
(26) Roy, G., Ananvoranich, S., and Perreault, J. P. (1999) Delta ribozyme has the ability to cleave in transan mRNA. *Nucleic Acids Res. 27*, 942−948.
(27) Yu, Y. C., Mao, Q., Gu, C. H., Li, Q. F., and Wang, Y. M. (2002) Activity of HDV ribozymes to trans-cleave HCV RNA. *World J. Gastroenterol. 8*, 694−698.
(28) Levesque, M. V., Levesque, D., Briere, F. P., and Perreault, J. P. (2010) Investigating a new generation of ribozymes in order to target HCV. *PLoS One 5*, e9627.
(29) Motard, J., Rouxel, R., Paun, A., von Messling, V., Bisaillon, M., and Perreault, J. P. (2011) A novel ribozyme-based prophylaxis inhibits influenza A virus replication and protects from severe disease. *PLoS One 6*, e27327.
(30) Lu, Y., Gu, J., Jin, D., Gao, Y., and Yuan, M. (2011) Inhibition of telomerase activity by HDV ribozyme in cancers. *J. Exp. Clin. Cancer Res. 30*, 1.
(31) Wang, C. X., Lu, Y. Q., Qi, P., Chen, L. H., and Han, J. X. (2010) Efficient inhibition of hepatitis B virus replication by hepatitis delta virus ribozymes delivered by targeting retrovirus. *Virol. J. 7*, 61.
(32) Robichaud, G. A., Perreault, J. P., and Ouellette, R. J. (2008) Development of an isoform-specific gene suppression system: the study of the human Pax-5B transcriptional element. *Nucleic Acids Res. 36*, 4609−4620.
(33) Fiola, K., Perreault, J. P., and Cousineau, B. (2006) Gene targeting in the Gram-Positive bacterium Lactococcus lactis, using various delta ribozymes. *Appl. Environ. Microbiol. 72*, 869−879.
(34) Peracchi, A. (2004) Prospects for antiviral ribozymes and deoxyribozymes. *Rev. Med. Virol. 14*, 47−64.
(35) Ferbeyre, G., Smith, J. M., and Cedergren, R. (1998) Schistosome satellite DNA encodes active hammerhead ribozymes. *Mol. Cell. Biol. 18*, 3880−3888.
(36) Martick, M., Horan, L. H., Noller, H. F., and Scott, W. G. (2008) A discontinuous hammerhead ribozyme embedded in a mammalian messenger RNA. *Nature 454*, 899−902.
(37) Herschlag, D., and Cech, T. R. (1990) Catalysis of RNA cleavage by the Tetrahymena thermophila ribozyme. 1. Kinetic description of the reaction of an RNA substrate complementary to the active site. *Biochemistry 29*, 10159−10171.
(38) Chadalavada, D. M., Gratton, E. A., and Bevilacqua, P. C. (2010) The human HDV-like CPEB3 ribozyme is intrinsically fast-reacting. *Biochemistry 49*, 5321−5330.
(39) Lupták, A., and Doudna, J. A. (2004) Distinct sites of phosphorothioate substitution interfere with folding and splicing of the Anabaena group I intron. *Nucleic Acids Res. 32*, 2272−2280.
(40) Hertel, K. J., Herschlag, D., and Uhlenbeck, O. C. (1994) A kinetic and thermodynamic framework for the hammerhead ribozyme reaction. *Biochemistry 33*, 3374−3385.
(41) Ananvoranich, S., Fiola, K., Ouellet, J., Deschenes, P., and Perreault, J. P. (2001) Kinetic analysis of bimolecular hepatitis delta ribozyme. *Methods Enzymol. 341*, 553−566.
(42) Rampasek, L., Jimenez, R. M., Luptak, A., Vinar, T., and Brejova, B. (2016) RNA motif search with data-driven element ordering. *BMC Bioinf. 17*, 216.
(43) Jimenez, R. M., Rampasek, L., Brejova, B., Vinar, T., and Lupták, A. (2012) Discovery of RNA motifs using a computational pipeline that allows insertions in paired regions and filtering of candidate sequences. *Methods Mol. Biol. 848*, 145−158.
(44) Sperschneider, J., and Datta, A. (2010) DotKnot: pseudoknot prediction using the probability dot plot under a refined energy model. *Nucleic Acids Res. 38*, e103.
(45) Hofacker, I. L. (2003) Vienna RNA secondary structure server. *Nucleic Acids Res. 31*, 3429−3431.


DOI: 10.1021/acs.biochem.7b00789
*Biochemistry* 2018, 57, 1440−1450

(46) Lupták, A., and Szostak, J. W. (2007) Mammalian self-cleaving ribozymes. In *Ribozymes and RNA catalysis* (Lilley, D. M. J., and Eckstein, F., Eds.) Royal Society of Chemistry, Cambridge, U.K.
(47) Been, M. D. (1994) Cis- and trans-acting ribozymes from a human pathogen, hepatitis delta virus. *Trends Biochem. Sci. 19*, 251−256.
(48) Lupták, A., Ferré-D'Amaré, A. R., Zhou, K., Zilm, K. W., and Doudna, J. A. (2001) Direct pK(a) measurement of the active-site cytosine in a genomic hepatitis delta virus ribozyme. *J. Am. Chem. Soc. 123*, 8447−8452.
(49) Fauzi, H., Kawakami, J., Nishikawa, F., and Nishikawa, S. (1997) Analysis of the cleavage reaction of a trans-acting human hepatitis delta virus ribozyme. *Nucleic Acids Res. 25*, 3124−3130.
(50) Kawakami, J., Yuda, K., Suh, Y. A., Kumar, P. K., Nishikawa, F., Maeda, H., Taira, K., Ohtsuka, E., and Nishikawa, S. (1996) Constructing an efficient trans-acting genomic HDV ribozyme. *FEBS Lett. 394*, 132−136.
(51) Hori, T., Guo, F., and Uesugi, S. (2006) Addition of an extra substrate binding site and partial destabilization of stem structures in HDV ribozyme give rise to high sequence-specificity for its target RNA. *Nucleosides, Nucleotides Nucleic Acids 25*, 489−501.
(52) Harris, D. A., Rueda, D., and Walter, N. G. (2002) Local conformational changes in the catalytic core of the trans-acting hepatitis delta virus ribozyme accompany catalysis. *Biochemistry 41*, 12051−12061.
(53) Pereira, M. J., Harris, D. A., Rueda, D., and Walter, N. G. (2002) Reaction pathway of the trans-acting hepatitis delta virus ribozyme: a conformational change accompanies catalysis. *Biochemistry 41*, 730−740.
(54) Jeong, S., Sefcikova, J., Tinsley, R. A., Rueda, D., and Walter, N. G. (2003) Trans-acting hepatitis delta virus ribozyme: catalytic core and global structure are dependent on the 5′ substrate sequence. *Biochemistry 42*, 7727−7740.
(55) Lee, C. B., Lai, Y. C., Ping, Y. H., Huang, Z. S., Lin, J. Y., and Wu, H. N. (1996) The importance of the helix 2 region for the cis-cleaving and trans-cleaving activities of hepatitis delta virus ribozymes. *Biochemistry 35*, 12303−12312.
(56) Bergeron, L. J., and Perreault, J. P. (2005) Target-dependent on/off switch increases ribozyme fidelity. *Nucleic Acids Res. 33*, 1240−1248.
(57) Bergeron, L. J., Reymond, C., and Perreault, J. P. (2005) Functional characterization of the SOFA delta ribozyme. *RNA 11*, 1858−1868.
(58) Shih, I., and Been, M. D. (2001) Energetic contribution of non-essential 5′ sequence to catalysis in a hepatitis delta virus ribozyme. *EMBO J. 20*, 4884−4891.
(59) Tinsley, R. A., and Walter, N. G. (2007) Long-range impact of peripheral joining elements on structure and function of the hepatitis delta virus ribozyme. *Biol. Chem. 388*, 705−715.
(60) Levesque, M. V., Rouleau, S. G., and Perreault, J. P. (2011) Selection of the most potent specific on/off adaptor-hepatitis delta virus ribozymes for use in gene targeting. *Nucleic Acid Ther. 21*, 241−252.
(61) Graf, S., Przybilski, R., Steger, G., and Hammann, C. (2005) A database search for hammerhead ribozyme motifs. *Biochem. Soc. Trans. 33*, 477−478.
(62) de la Pena, M., and Garcia-Robles, I. (2010) Ubiquitous presence of the hammerhead ribozyme motif along the tree of life. *RNA 16*, 1943−1950.
(63) de la Pena, M., and Garcia-Robles, I. (2010) Intronic hammerhead ribozymes are ultraconserved in the human genome. *EMBO Rep. 11*, 711−716.
(64) Jimenez, R. M., Delwart, E., and Lupták, A. (2011) Structure-based search reveals hammerhead ribozymes in the human microbiome. *J. Biol. Chem. 286*, 7737−7743.
(65) Perreault, J., Weinberg, Z., Roth, A., Popescu, O., Chartrand, P., Ferbeyre, G., and Breaker, R. R. (2011) Identification of hammerhead ribozymes in all domains of life reveals novel structural variations. *PLoS Comput. Biol. 7*, e1002031.
(66) Seehafer, C., Kalweit, A., Steger, G., Graf, S., and Hammann, C. (2011) From alpaca to zebrafish: hammerhead ribozymes wherever you look. *RNA 17*, 21−26.
(67) Roth, A., Weinberg, Z., Chen, A. G. Y., Kim, P. B., Ames, T. D., and Breaker, R. R. (2014) A widespread self-cleaving ribozyme class is revealed by bioinformatics. *Nat. Chem. Biol. 10*, 56−U92.
(68) Ananvoranich, S., and Perreault, J. P. (1998) Substrate specificity of delta ribozyme cleavage. *J. Biol. Chem. 273*, 13182−13188.
(69) Freier, S. M., Kierzek, R., Jaeger, J. A., Sugimoto, N., Caruthers, M. H., Neilson, T., and Turner, D. H. (1986) Improved free-energy parameters for predictions of RNA duplex stability. *Proc. Natl. Acad. Sci. U. S. A. 83*, 9373−9377.
(70) Hertel, K. J., Peracchi, A., Uhlenbeck, O. C., and Herschlag, D. (1997) Use of intrinsic binding energy for catalysis by an RNA enzyme. *Proc. Natl. Acad. Sci. U. S. A. 94*, 8497−8502.
(71) Narlikar, G. J., Gopalakrishnan, V., McConnell, T. S., Usman, N., and Herschlag, D. (1995) Use of binding energy by an RNA enzyme for catalysis by positioning and substrate destabilization. *Proc. Natl. Acad. Sci. U. S. A. 92*, 3668−3672.
(72) Bevilacqua, P. C., Li, Y., and Turner, D. H. (1994) Fluorescence-detected stopped flow with a pyrene labeled substrate reveals that guanosine facilitates docking of the 5′ cleavage site into a high free energy binding mode in the Tetrahymena ribozyme. *Biochemistry 33*, 11340−11348.
(73) Riccitelli, N. J., and Lupták, A. (2010) Computational discovery of folded RNA domains in genomes and in vitro selected libraries. *Methods 52*, 133−140.
(74) Jimenez, R. M., and Lupták, A. (2012) Structure-based search and in vitro analysis of self-cleaving ribozymes. *Methods Mol. Biol. 848*, 131−143.
(75) Gruber, A. R., Lorenz, R., Bernhart, S. H., Neubock, R., and Hofacker, I. L. (2008) The Vienna RNA websuite. *Nucleic Acids Res. 36*, W70−74.


DOI: 10.1021/acs.biochem.7b00789
*Biochemistry* 2018, 57, 1440−1450